

Communication

Not peer-reviewed version

Raman Study of Novel Walls-like Nanostructured WO₃ Thin Films Grown by Spray Deposition

[Andreea Gabriela Marina Popescu](#) , Ioan Valentin Tudose , [Cosmin Romanitan](#) , Marian Popescu , [Marina Manica](#) , Paul Schiopu , [Mirela Petruta Sucheai](#) ^{*} , [Cristina Pachiui](#) ^{*}

Posted Date: 7 June 2024

doi: 10.20944/preprints202406.0431.v1

Keywords: Raman spectroscopy; tungsten oxide; spray pyrolysis; thin films



Preprints.org is a free multidiscipline platform providing preprint service that is dedicated to making early versions of research outputs permanently available and citable. Preprints posted at Preprints.org appear in Web of Science, Crossref, Google Scholar, Scilit, Europe PMC.

Copyright: This is an open access article distributed under the Creative Commons Attribution License which permits unrestricted use, distribution, and reproduction in any medium, provided the original work is properly cited.

Communication

Raman Study of Novel Walls-like Nanostructured WO₃ Thin Films Grown by Spray Deposition

Andreea Popescu ^{1,2}, Ioan Valentin Tudose ^{3,4}, Cosmin Romanitan ¹, Marian Popescu ¹, Marina Manica ¹, Paul Schiopu ², Mirela Petruta Sucnea ^{1,3,*} and Cristina Pachiu ^{1,*}

¹ National Institute for Research and Development in Microtechnologies - IMT Bucharest, 126A, Erou Iancu Nicolae Street, 077190, Voluntari-Bucharest, Romania; popescu96andreea@gmail.com (A.P.); cosmin.romanitan@imt.ro (C.R.); manicamarina7@gmail.com (M.M.)

² Doctoral School of Electronics, Telecommunications and Information Technology, National University of Science and Technology POLITEHNICA Bucharest, 061071, Bucharest, Romania; schiopu.paul@yahoo.com

³ Center of Materials Technology and Photonics, School of Engineering, Hellenic Mediterranean University, 71410 Heraklion, Crete, Greece; tudose_valentin@yahoo.com

⁴ Chemistry Department, University of Crete, Heraklion, Greece

* Correspondence: mirasucnea@hmu.gr or mira.sucnea@imt.ro (M.P.S.); cristina.pachiu@imt.ro (C.P.)

Abstract: Walls-like structured monoclinic WO₃ thin films were obtained by spray deposition method for further integration in gas sensors. For sensing applications, it is very important to achieve a high surface-to-volume ratio surface together with a proper thin films structure. The present communication reports on the effect of the sprayed solution volume variation (as a thickness variation element) on the detailed Raman spectroscopy for WO₃ thin films with different thicknesses grown from precursor solutions with two different concentrations. Detailed analysis of the two series of samples shows that the growing thickness strongly affects the films morphology while their crystalline structure is only slightly affected. The Raman analysis contribute to refining the structural features clarifications. It was observed that, for both concentrations, the increase in thickness seems to slightly affect the stoichiometry of material and, in association with surface morphology variations, provide new possibilities for fine tuning of films properties towards enhanced as sensing applications. Further studies are ongoing.

Keywords: Raman spectroscopy; tungsten oxide; spray pyrolysis; thin films

1. Introduction

The response and performance of sensor devices are critically influenced by several factors, including the size, shape, and surface characteristics of the active oxide material. These attributes play a crucial role in defining the electronic and optical properties of oxides, which are known to vary significantly with spatial dimensions and composition. Among the various forms that these materials can take, thin films have emerged as one of the most effective configurations for achieving high sensitivity in sensors. This heightened sensitivity is primarily due to the increased number of surface atoms present in thin films, which enhances their interaction with the surrounding environment. The physical and chemical properties of the nano-structured sensing layer, such as tungsten oxide (WO₃), are notably different from those of their bulk counterparts. This disparity arises because the large surface area to volume ratio in nanostructures intensifies surface effects. In nano-scale dimensions, the effective van der Waals forces, Coulombic interactions, and inter-atomic couplings are significantly altered compared to the bulk material. These modified interactions lead to changes in the electronic structure and chemical reactivity of the material. Specifically, the high surface area in thin films means that a larger proportion of the atoms are exposed to the environment, which can enhance the sensitivity of the sensor. The increased surface interactions enable the material to

respond more readily to external stimuli, such as changes in gas concentration, temperature, or light. Furthermore, the reduced dimensionality in thin films can result in quantum confinement effects, which can further modify the electronic properties of the material, leading to improved performance in applications like gas sensing, photodetectors, and other optoelectronic devices. The ability to tailor the properties of the oxide material by manipulating its size, shape, and surface characteristics opens new possibilities for designing sensors with enhanced performance. For example, by optimizing the thickness of WO_3 thin films and controlling their nanostructure, it is possible to achieve a balance between high sensitivity and stability, which is crucial for practical sensor applications. The interplay between surface atoms and the altered inter-atomic forces in these nanostructured films provides a rich field of study for developing advanced materials with superior sensing capabilities. The performance of sensor devices is intricately linked to the characteristics of the active oxide material, particularly in its nano-structured thin film form. The unique properties that arise from the high surface area and modified inter-atomic interactions in these materials pave the way for highly sensitive and efficient sensors, making thin films a preferred choice in the design of next-generation sensing technologies.

WO_3 is a typical n-type gas-sensing material that attracted considerable attention and it is used to detect various hazardous gases. Previous studies indicated that unique nanostructuring during growth is highly related to the sensing performances. Countless advances have been achieved to design and fabricate diverse WO_3 in different forms. However, it is still challenging to achieve high performances. To significantly enhance the gas-sensing properties, many strategies have been explored. Although the mechanisms responsible for WO_3 gas sensing are not completely understood, an empirical model to explain the fundamental gas sensing mechanism is widely accepted as follows. Upon exposing to air, oxygen molecules will be chemisorbed on the WO_3 surface, inducing the creation of an electron depletion layer by attracting electrons from conduction band. The adsorbed oxygen can further evolve into active oxygen species such as O_2^- , O^- , and O^{2-} at a certain temperature [2], which is highly reactive with target gas molecules. The charge carriers are affected by the presence of target gas. For example, a reduction reaction can occur between reducing gases and these oxygen species, leading to the release of the trapped electrons back. As a result, the change in resistance reflects the concentrations of target gas. In the past years, typical 2D WO_3 structures such as thin films have drawn considerable attention in the gas-sensing field due to the high surface-to-volume ratio, modulated surface activities, surface polarization and rich oxygen vacancies. Many studies on WO_3 use as sensing layers are present in the scientific literature but this material is still challenging [3,4]. Raman spectroscopy can detect different stoichiometries and structures, including polymorphs that contain the same atoms but in different crystalline forms. This technique allows for the analysis of mixtures and the quantification of their chemical composition. Despite the extensive research on WO_3 thin films, a Raman spectroscopy study examining the effects of thickness variations correlated with the initial concentration of the precursor has, to our knowledge, not been performed before. This specific investigation is important as it could provide new insights into how these variables influence the material's structural and chemical properties, which are critical for optimizing its performance in various applications. By leveraging Raman spectroscopy, one can detect subtle changes in the WO_3 thin films' structure and composition induced by varying thickness and precursor concentration. This method's sensitivity to different stoichiometries and crystalline forms makes it particularly suited for such an analysis. Therefore, conducting this study could potentially uncover novel information about the interplay between film thickness, precursor concentration, and the resultant properties of WO_3 thin films. This could lead to improved methodologies for fabricating thin films with tailored properties for specific technological applications. The scope of the present study is to observe and correlate structural properties characterized by Raman spectroscopy for two kinds of pure WO_3 nanostructured thin films thickness series grown from precursors with two different concentrations leading to a rare structuring of the surface, only briefly noticed in the scientific literature. As mentioned above, up to our knowledge, a Raman spectroscopy study of the thickness variations effect correlated with initial concentration of precursor was never performed before on WO_3 thin films. This is a specific niche in materials science research. While WO_3 thin films and their properties

have been extensively studied, the unique combination of variables—thickness variation and initial precursor concentration, specifically analyzed through Raman spectroscopy is novel.

2. Materials and Methods

WO₃ thin films' deposition was performed using a custom-made air carrier flow static spray pyrolysis device. The films' growth was carried out at a vertical position and at a 30 cm distance between the spray nozzle and the substrate, which was kept at a temperature of 250°C during deposition. The precursor solution was prepared by dissolving the required amount of tungstic acid H₂WO₄ in distilled water for obtaining 0.1 M and 0.05 M solutions. Three different quantities (5, 8 and 12 mL) were employed, since the thickness of the films can be controlled by the volume of the solution. Thickness could not be measured to an accurate level due to the complex surface morphology of the films. The growth time increased with increase in the volume of solution, while the flow of the air carrier remained constant to ensure a constant deposition rate. Tungstic acid (H₂O₄W), ≥99.0% (calcined substance, T) powder was purchased from Sigma-Aldrich (Sigma-Aldrich, St. Louis, MO, USA) and distilled water was used as a solvent for the precursor's preparation. Fluorine-doped Tin Oxide (FTO – F:SnO₂) coated glass was the substrate. After the spray deposition of the thin films, thermal annealing was carried out for 2 h at 450°C in oxygen atmosphere.

X-ray diffraction (XRD, Rigaku, Tokyo, Japan) was performed using a Rigaku ultra high-resolution triple axis multiple reflection SmartLab X-ray Diffraction System, Tokyo, Japan. Scanning electron microscopy (SEM) characterization was done using a field emission Nova NanoSEM 630 (FEI Company, Hillsborough, OR, USA) and a field emission scanning electron microscope (FE-SEM) without sample preparation. Detailed Raman spectroscopy analysis was carried out using a Witec Raman spectrometer (Alpha-SNOM 300 S, WiTec GmbH, Ulm, Germany). Raman spectroscopy was performed to observe and correlate phase purity and structural properties of the WO₃ films under a visible (532 nm) laser excitation using the Witec Raman spectrometer equipped with a confocal microscope (Olympus 100x) and the visible excitation generated by a Nd-YAG doubled diode pumped laser with output power of 50 mW. The Raman spectra of the tungsten oxide were taken under ambient conditions with the spectral acquisition time 20 s/scan.

3. Results and Discussions

SEM imaging at low-magnification was conducted on six samples selected upon the precursor's volumes and concentrations: 5, 8, 12 ml at 0.1 M and 0.05 M. The SE images displayed in **Figure 1** disclose significant morphological variations on large areas of the WO₃ layer, as seen below:

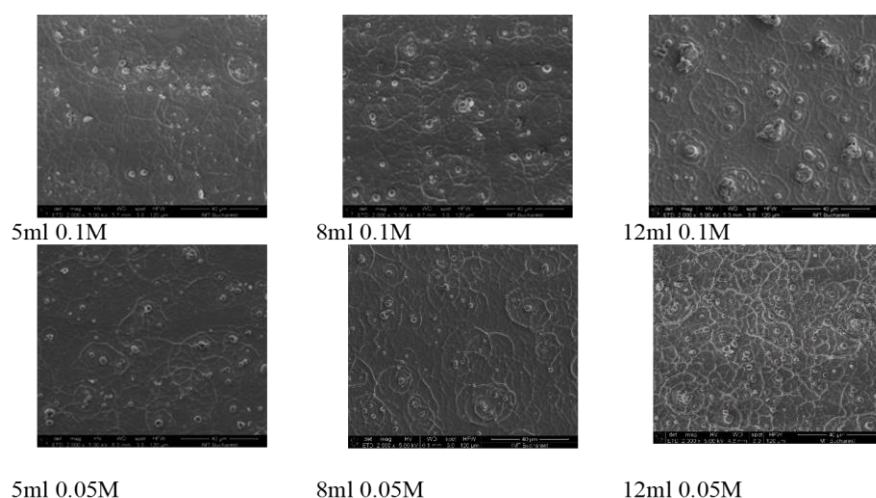


Figure 1. SEM images of WO₃ thin films grown at precursor's volumes and concentrations: 5, 8, 12 ml at 0.1 M and 0.05 M.

It can be observed that for a specific precursor concentration, the increasing thickness leads to a surface morphology with increased number of features. It is observed the presence of small islands alternating with walls like structures with size increasing as the thickness increases. With respect to the precursor concentration, higher molar concentration for the precursor solution leads to similar surface morphology at small thickness but, as the thickness increases the surface morphologies changes and, at lower precursor concentration a higher number of wall-like structures appears while the island like structures number and size decreases. At higher precursor concentration, the surface morphology seems to evolve towards larger islands-like structures as the thickness is increasing.

Grazing incidence X-ray diffraction was employed to study the constituent phases of WO_3 films. For this purpose, the incidence angle was kept at 0.5° , while the detector scanned in the 2θ range of $20 - 60^\circ$ as shown in Figure 2.

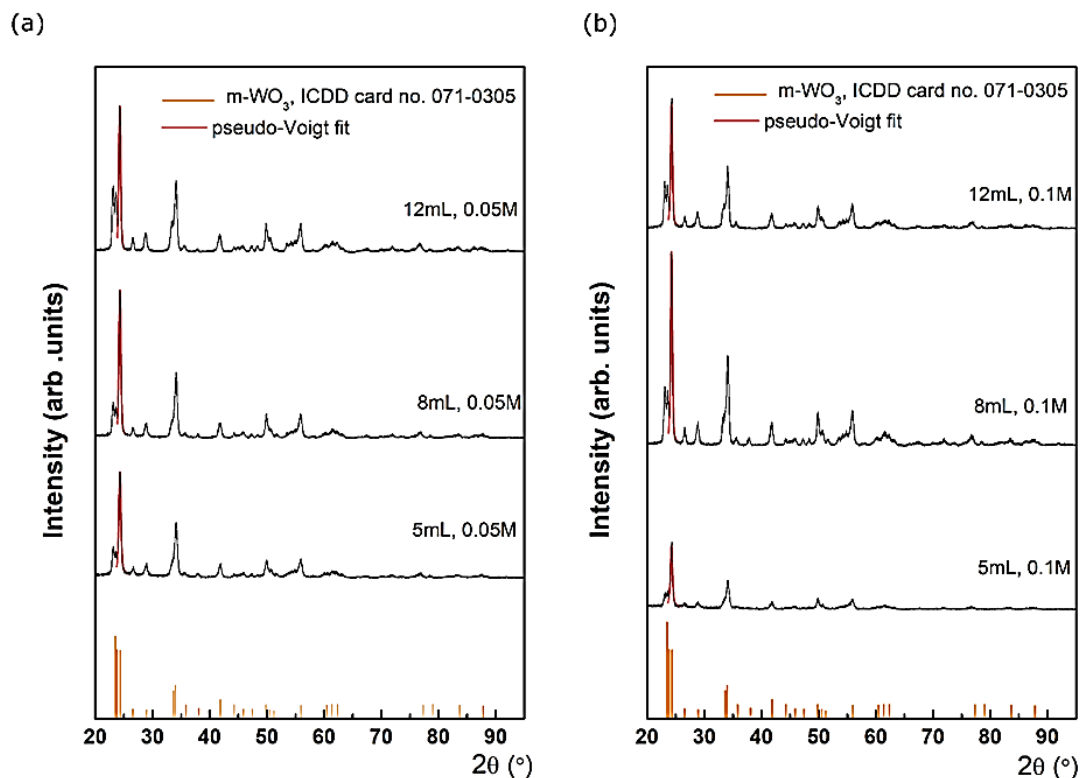


Figure 2. XRD patterns of WO_3 thin films grown at precursor's volumes and concentrations: 5, 8, 12 ml at 0.1 M and 0.05 M.

The XRD data reveal the presence of single phase WO_3 . Each diffraction pattern presents a set of diffraction features with different intensities located at $23.1, 23.5, 24.2, 26.5, 28.7, 33.3, 34.1, 35.4, 41.7, 44.4, 45.6, 47.2, 48.3, 49.9, 50.7$ and 55.8° , assigned with different (hkl) Miller indices using ICDD database – International Center for Diffraction Data. These were attributed to WO_3 with monoclinic crystal structure, belonging to $P2_1/n(14)$ space group with the following lattice parameters and angles: $a = 0.73 \text{ nm}$; $b = 0.75 \text{ nm}$; $c = 0.76 \text{ nm}$; $\alpha = 90^\circ$; $\beta = 90.9^\circ$; $\gamma = 90^\circ$, according to card no. 05-0363. No impurities peaks were detected in the XRD patterns. A monoclinic phase was also observed by different authors. For instance, Dongale and co-workers [5] reported monoclinic WO_3 films obtained using spray pyrolysis at different substrate temperatures. Acosta et al. [6] reported monoclinic phase of WO_3 with a preferred orientation of the crystallites along the c-axis, while Ortega et al. [7] showed the hexagonal and monoclinic phase co-existence on glass substrate and a pure monoclinic phase on FTO for WO_3 deposited by pulsed spray pyrolysis. In addition, multiple reports related to the WO_3 films and nanostructures exhibit monoclinic crystal structures [8; 9; 10]. Different deposition parameters do not affect the position of the diffraction peaks, which indicates that the interplanar

distance of the monoclinic-WO₃ remains constant along different precursor's volume and concentration. However, the fitting of the main diffraction peaks located at 24.3°, with a pseudo-Voigt function indicates that the crystal quality is affected at different deposition parameters. For instance, at 0.05M for the lowest precursor's volume (5mL), the Full Width at Half Maximum (FWHM) of the main diffraction peak is 0.51°. Further, when the precursor's volume increases, the FWHM decreases to 0.46° (8 mL), reaching to 0.45° (12 mL). Similarly, at 0.1 M, the FWHM decreases from 0.51° (5 mL) to 0.43° (8 and 12 mL). According to Scherrer equation [11], with increasing the precursor's volume, the crystal quality becomes better, which is reflected in the mean crystallite size increases from ~ 16 nm to ~ 19.5 nm. These observations are supported by the Raman spectroscopy characterization that follows.

Raman spectroscopy results for the WO₃ thin films grown at precursor's volumes and concentrations: 5, 8, 12 ml at 0.1 M and 0.05 M are presented in Figure 3.

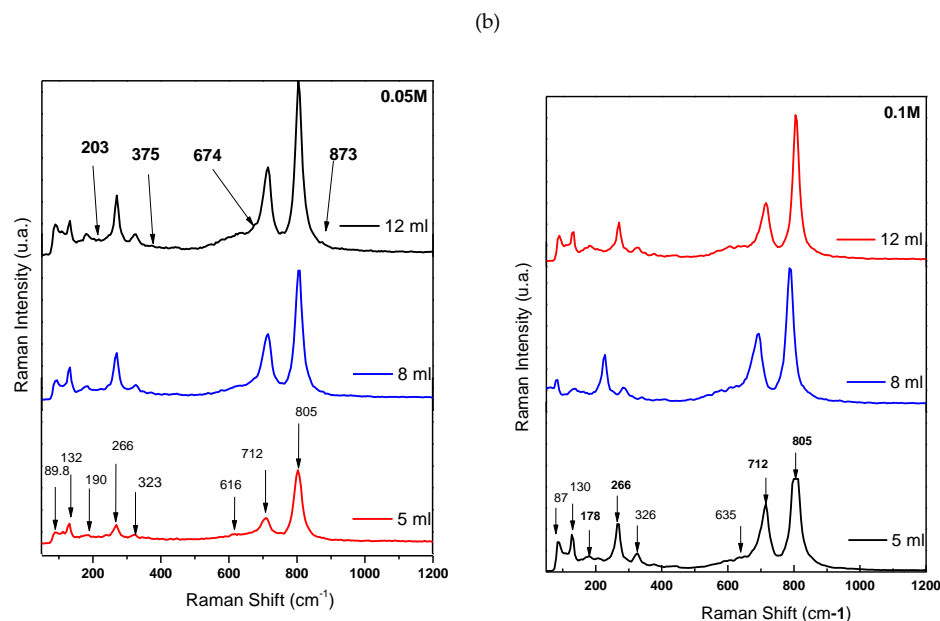


Figure 3. Raman spectroscopy results for WO₃ thin films grown at precursor's volumes and concentrations: 5, 8, 12 ml at a 0.05 M and b 0.1 M.

As already mentioned, Raman spectroscopy offers important information about the crystalline phases of WO₃ crystal. Tungsten trioxide thin films can exist in different phases depending on synthesis temperature (a) low-temperature phase (m-WO₃) - this is the most stable phase of WO₃ at ambient conditions corresponding to the monoclinic crystal structure. The α -phase can be synthesized at relatively low temperatures, typically below 740°C [12]; (b) high-temperature phase (- at higher temperatures, typically above 740°C, α -WO₃ transforms into the c-phase a cubic (ideal) crystal structure; (c) the phase transitions in the WO₃ thin films occur in sequence as the temperature is increased: monoclinic (α -WO₃) --> orthorhombic (β -WO₃) --> tetragonal phase (α -WO₃) [13].

For sensing functions, the WO₃ needs to be nanostructured and have a large surface area to enable the analytes to diffuse through the film. Acentric nature and spontaneous electric dipole moment of ferroelectric ϵ -WO₃ for example, leads to increased interaction with high dipole moment analytes such as acetone [14] which is used for medical devices sensing the acetone level in human breath in concentrations of parts per billion (ppb) for non-invasive blood glucose monitoring [15]. In the monoclinic phase, photo electrochemical and photo catalytic properties are enhanced when the film is highly crystalline and preferentially oriented because this highly crystalline structure will have fewer defects when acting as the recombination center and should suppress mutual e⁻-h⁺ recombination [16]. According to some authors, polycrystalline WO₃ film has almost no

photochromic sensitivity whereas amorphous WO₃ has high photochromic and electrochromic sensitivity due to high surface area [17].

The fundamental Raman vibrational modes within the lattice of WO₃ contain stretching (ν), bending (δ), and out-of-plane wagging (γ) modes.

In the monoclinic m-WO₃ crystalline structure, these vibration modes are observed at \approx 803, 714, and 270 cm⁻¹, corresponding to the stretching of ν (O-W-O) bonds, stretching of ν (W-O) bonds, and bending of δ (O-W-O) bonds, respectively [18].

Comparing the Raman spectra (Figure 3) obtained for WO₃ films made by spray deposition method with results reported in the literature using other deposition techniques (Chemical Vapor Deposition, Chemical Solution Deposition, or Dip-Coating), one can observe a dominant presence of vibration modes at 270 cm⁻¹, 714 cm⁻¹, and 805 cm⁻¹. This indicates a monoclinic structure of m-WO₃ but with changes in the Raman spectrum of the resulting material induced by the deposition method.

The O-W-O and W-O bonds in monoclinic structure remain unchanged, with variations only in intensity when the increase in volume for spray-coating (for 0.5 M δ (O-W-O), I12 ml/I5ml= 1.96) and are less sensitive to higher molar masses (for 0.1 M δ (O-W-O), I12 ml/I5ml = 0.15).

The WO₃ Raman spectra (Figure 3a – 0.05 M probes) displays bands at low wavenumbers, observed within the wavenumber range of 80 - 400 cm⁻¹. Above all, Figure 3b – 0.1 M probe with bands identification, there is a cluster of bands at 89,131, 190, and 266 cm⁻¹. The bands below 270 cm⁻¹ are attributed to low frequency phonon charge marker. The band at 266 cm⁻¹ is attributed to lattice modes ν (O-W-O) vibration, the other bands correspond to W-W lattice modes vibration. At the same time, the Raman bands corresponding to the W-W bonding located in the 200 cm⁻¹ region become more intense, being closely related to the increased structural order in the spray-deposited WO₃ material (Figure 4, 12 ml volume sprayed).

The bands between 270 and 700 cm⁻¹ are the typical modes indicating the crystalline quality of the WO₃ films [19].

In this case, the deposition process influenced the crystalline structure of WO₃, altering the vibration mode of certain atomic bonds in the material such as a weak δ (O-W-O), reflected through weak vibration modes in the Raman spectrum (Figure 3), as well as the weak presence of O-lattice bonds in the spectral region around 600 cm⁻¹ (absence of predominant O-lattice modes at frequencies of approx. 604 and 674 cm⁻¹ – table 1). All these changes are induced by deviations from the ideal stoichiometry of the WO₃ composition, resulting in a variation of the atomic ratio between tungsten and oxygen

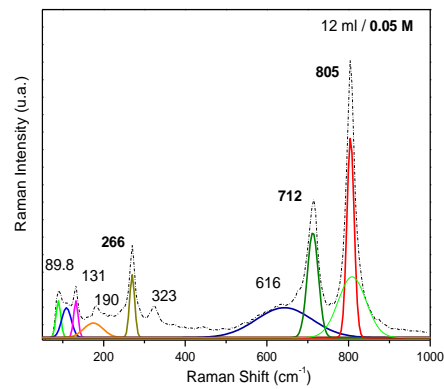
The bond at 714 cm⁻¹, also known as the γ (W-O) band, in the Raman spectrum of WO₃, indicates the vibrations of tungsten atoms bonded to oxygen atoms in the crystalline lattice. The disappearance of this band may be associated with the loss of some oxygen atom bonds in the crystal lattice.

The band at 806 cm⁻¹ represents the Raman vibration mode of crystalline WO₃ (m-phase), indicating the stretching vibrations of the bridging oxygen, ν_a (O-W-O).

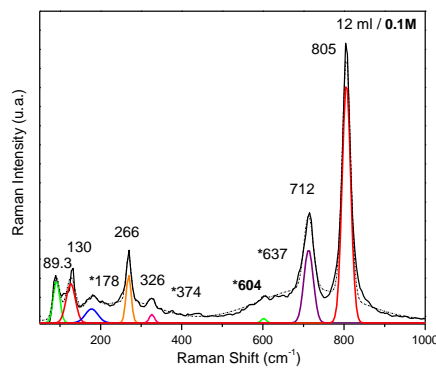
The disappearance of symmetric ν_s (O-W-O) may be caused by chemical reactions leading to modification or destruction of terminal oxygen groups in the WO₃ lattice. This could result from interactions with compounds during the deposition process.

Table 1. Summary of WO₃ Raman bands.

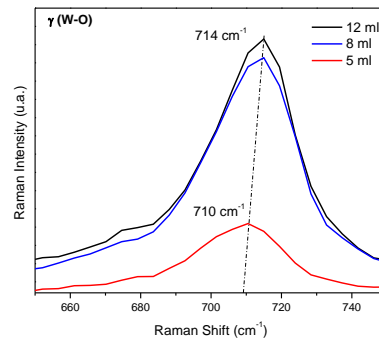
Raman band (cm ⁻¹)	Raman assignment
89.73	low frequency phonon change marker
110.83	low frequency phonon change marker
180	low frequency phonon change marker
203.89	W-W
270.02	ν (O-W-O) in monoclinic phase
326.31	δ (O-W-O)
374	δ (O-W-O)
604	O-lattice
674	O-lattice
714.96	γ (W-O)
803.91	ν_a (anti symmetric O-W-O) monoclinic phase
873	ν_s (symmetric W=O terminal)



a



b



c

Figure 4. **a** and **b** -examples of the deconvoluted Raman spectra of the 12mL WO₃ at the two different concentrations; **c** – Raman intensity variation with Raman shift for the films with different thickness.

Deposition of WO₃ by spray-coating induces slight shifts in the frequency of the Raman bands (Figure 4c γ (W-O)). These shifts may be caused by changes in the local environment of the tungsten atoms or alterations in the interactions between atoms and light.

Another consequence of using the spray deposition process seems to be the decrease in FWHM Raman modes: FWHM for ν (O-W-O) mode for 5 ml decrease with $\approx 12\%$, the same behavior is observed for the modes γ (W-O) and ν_a (O-W-O) as well.

All these changes in the Raman spectrum of the spray-deposited material may be associate with the improved crystallization of the material and a reduction in the dispersion of vibration modes in the WO₃ crystalline structure. The detailed Raman spectroscopy analysis of spray-deposited WO₃ films provides a comprehensive understanding of structural characteristics, crystalline properties, and the influence of deposition parameters on material quality. These insights are crucial for

optimizing WO₃-based sensors and other applications requiring precise control over material structure and properties.

5. Conclusions

Using spray deposition method, walls-like structured monoclinic WO₃ thin films were obtained by for further integration in gas sensors. As for sensing applications it is very important to achieve a high surface-to-volume ratio surface together with a proper thin films structure and stoichiometry, the WO₃ thin films developed during this work seems to offer excellent premises for use as sensing layers. The effect of the sprayed solution volume variation (as a thickness variation element) on the detailed Raman spectroscopy for WO₃ thin films with different thicknesses grown from precursor solutions with two different concentrations was analyzed. Detailed analysis of the two series of samples showed that the growing thickness strongly affects the films morphology while their crystalline structure is only slightly affected. The Raman analysis contribute to refining the structural observations by XRD. It was observed that, for both concentrations, the increase in thickness seems to slightly affect the stoichiometry of material and, in association with surface morphology variations, provide new possibilities for fine tuning of films properties towards enhanced as sensing applications. Furter studies are ongoing.

Author Contributions: Conceptualization, M.P.S. and I.V.T.; Data curation, M.P.S. and I.V.T.; Formal analysis, and M.P.S.; Funding acquisition, M.P.S.; Investigation, A.P., I.V.T., C.R., M.P., M.M., P.S., and C.P.; Methodology, M.P.S. and I.V.T.; Project administration, M.P.S. and I.V.T.; Resources, C.P. and M.P.S.; Supervision, M.P.S., P.S., Validation, M.P.S. and I.V.T.; Visualization, A.P., C.R., M.P., M.M. and C.P.; Writing—original draft, A.P., I.V.T., C.R., M.P., M.M., P.S., and C.P.; Writing—review and editing, C.P. and M.P.S. All authors have read and agreed to the published version of the manuscript.

Funding: This research received no external funding.

Data Availability Statement: The raw and processed data required to reproduce these findings cannot be shared at this time due to technical or time limitations. The raw and processed data will be provided upon reasonable request until the technical problems have been solved.

Acknowledgments: IMT's contribution was partially supported by the "MicroNEx", Contract nr. 20 PFE /30.12.2021, financed by the Ministry of Research, Innovation and Digitization through Program 1—Development of the National R & D System, Subprogram 1.2—Institutional Performance—Projects for Institutional Excellence, Romanian Ministry of Research, Innovation and Digitalisation through the μ NanoEI, Cod: 23 07 core Programme, and partially supported by PNRR/2022/C9/MCID/I8 CF23/14 11 2022 contract 760101/23.05.2023 financed by the Ministry of Research, Innovation and Digitalization in "Development of a program to attract highly specialized human resources from abroad in research, development, and innovation activities" within the – PNRR-IIIC9-2022 - I8 PNRR/2022/Component 9/investment 8.

Conflicts of Interest: The authors declare no conflicts of interest. The funders had no role in the design of the study; in the collection, analyses, or interpretation of data; in the writing of the manuscript; or in the decision to publish the results.

References

1. Rogers, B.; Adams, J.; Pennathur S. Nanotechnology: Understanding Small Systems, 3rd ed.; Publisher: CRC Press, Taylor & Francis Group, New York. 2015.
2. Das S.; Jayaraman, V. SnO₂: A comprehensive review on structures and gas sensors, Progress in Materials Science 2014, Volume 66, pages 112-255.
3. Dong, C.; Zhao, R.; Yao, L.; Ran, Y.; Zhang, X.; Wang, Y. A review on WO₃ based gas sensors: Morphology control and enhanced sensing properties. Journal of Alloys and Compounds 2020, Volume 820, page 153194.
4. Li, X.; Fu, L.; Karimi-Maleh, H.; Chen F.; S. Zhao, S. Innovations in WO₃ gas sensors: Nanostructure engineering, functionalization, and future perspectives. Heliyon 2024, Volume 10, page 27740.
5. Dongale, T.D.; Mohite, S.V.; Bagade, A.A.; Gaikwad, P.; Patil, P.S.; Kamat, R.K.; Rajpure, K. Development of Ag/WO₃/ITO Thin Film Memristor Using Spray Pyrolysis. Method. Electron. Mater. Lett. 2015, Volume 11, page 944–948.

6. Acosta, D. R.; Magaña, C.; Hernández, F.; Ortega J. Electrical, optical and electrochromic properties of Ti:WO₃ thin films deposited by the pulsed chemical spray technique. *Thin Solid Films* 2015, Volume 594, pages 207-214.
7. Ortega, J.M.; Martínez, A.I.; Acosta, D.R.; Magaña C.R. Structural and electrochemical studies of WO₃ films deposited by pulsed spray pyrolysis, *Solar Energy Materials and Solar Cells* 2006, Volume 90, pages 2471-2479.
8. Sivakumar, R.; Moses Ezhil Raj, A.; Subramanian, B.; Jayachandran, M.; Trivedi, D.C.; Sanjeeviraja C. Preparation and characterization of spray deposited n-type WO₃ thin films for electrochromic devices, *Materials Research Bulletin* 2004, Volume 39, pages 1479-1489.
9. Kolhe, P.S.; Mutadak, P.; Maiti, N.; Sonawane K.M. Synthesis of WO₃ nanoflakes by hydrothermal route and its gas sensing application. *Sensors and Actuators A: Physical* 2020, Volume 304, page 111877.
10. Hunge, Y.M.; Yadav, A.A.; Mahadik, M.A.; Mathe, V.L.; Bhosale, C.H. A highly efficient visible-light responsive sprayed WO₃/FTO photoanode for photoelectrocatalytic degradation of brilliant blue, *Journal of the Taiwan Institute of Chemical Engineers* 2018, Volume 85, pages 273-281.
11. Patterson, A.L. The Scherrer Formula for X-Ray Particle Size Determination, *Phys. Rev.* 1939, Volume 56
12. Salje, E.; Viswanathan, K. Physical properties and phase transitions in WO₃, *Acta Cryst.* 1975, Volume A31, pages 356-359.
13. Han, W.; Qian Shi, Q.; Hu, R. Advances in Electrochemical Energy Devices Constructed with Tungsten Oxide-Based Nanomaterials, *Nanomaterials* 2021, Volume 11(3), page 692.
14. Woodward, P.M.; Sleight, A.W.; Vogt, T. Ferroelectric Tungsten Trioxide, *Journal of Solid State Chemistry* 1997, Volume 131, pages 9-17.
15. Wang, L.; Kalyanasundaram, K.; Stanacevic, M.; Gouma, P. Nanosensor Device for Breath Acetone Detection, *Sensor Letters* 2010, Volume 8(5), page 709-712.
16. Liu, J.; Dong, X.; Li X.W.; Shi, F. Solvothermal synthesis and characterization of tungsten oxides with controllable morphology and crystal phase, *Journal of Alloys and Compounds* 2011, Volume 509(5), page 1482-1488.
17. R. Jain, R.; Wang, Y.; Maric, R. Tuning of WO₃ Phase Transformation and Structural Modification by Reactive Spray Deposition Technology, *J Nanotech Smart Mater* 2014, Volume 1, page 203.
18. Adu, K.W.; Xiong, Q.; Gutierrez, H.R.; Chen, G.; Eklund, P.C. Raman scattering as a probe of phonon confinement and surface optical modes in semiconducting nanowires, *Applied Physics A* 2006, Volume 85, pages 287-297.
19. Bertus, L.M.; Faure, C.; Danine, A.; Labrugere, C.; Campet, G.; Rougier, A.; Duta, A. Synthesis and characterization of WO₃ thin films by surfactant assisted spray pyrolysis for electrochromic applications *Materials Chemistry and Physics* 2013, Volume 140, pages 49-59.

Disclaimer/Publisher's Note: The statements, opinions and data contained in all publications are solely those of the individual author(s) and contributor(s) and not of MDPI and/or the editor(s). MDPI and/or the editor(s) disclaim responsibility for any injury to people or property resulting from any ideas, methods, instructions or products referred to in the content.